HOKKAIDO UNIVERSITY

Title	Heme Iron Coordination Structure of Heme Transport Protein HutB from Vibrio Cholerae
Author(s)	Uchida, Takeshi; Funamizu, Takumi; Ogura, Mariko; Ishimori, Koichiro
Citation	Bulletin of the Chemical Society of Japan, 90(8), 924-930 https://doi.org/10.1246/bcsj.20170104
Issue Date	2017-08
Doc URL	http://hdl.handle.net/2115/68744
Type	article
File Information	bcsj_HutB.pdf

Instructions for use

Heme iron coordination structure of heme transport protein HutB from *Vibrio cholerae*

Takeshi Uchida[1,2], Takumi Funamizu[2], Mariko Ogura[2], and Koichiro Ishimori[1,2]

[1]Department of Chemistry, Faculty of Science, Hokkaido University, Sapporo 060-0810, Japan

[2]Graduate School of Chemical Sciences and Engineering, Hokkaido University, Sapporo 060-8628, Japan

E-mail: <uchida@sci.hokudai.ac.jp>

Takeshi Uchida
Takeshi Uchida received Ph.D. degree from Kyoto University in 1998. He began his academic career at Institute for Molecular Science, and then became an Associate Professor of Hokkaido University in 2013. His research interests are reaction mechanism and structural analysis of metalloenzymes.

Abstract

HutB is a putative heme transport protein located in the periplasmic space in *Vibrio cholerae*. Here, we purified HutB and characterized its heme binding properties. An analysis of the Soret band showed that there are two types of heme binding geometries depending on the heme concentration: 404-nm species are dominant at lower concentrations of heme, and 394-nm species dominate at higher concentrations. Moreover, a mutational study revealed that either Tyr65 or Tyr198 binds heme with the help of histidine, a property shared with another *V. cholerae* heme transport protein, HutX, despite the absence of sequence similarity, indicating that HutB acts as a heme transport protein in the periplasm.

1. Introduction

Iron is an essential element for the growth of bacteria because it is present as a cofactor in many proteins that play key roles in metabolic processes, such as electron transfer and energy transduction. Bacteria have evolved two sophisticated iron acquisition systems for obtaining iron: siderophores and heme-uptake systems.[1,2] Siderophores are secreted low-molecular-weight compounds that bind ferric iron from many iron sources, such as soil, water and transferrin, with high affinity.[3] Iron-bound siderophores are taken up through receptor proteins in the outer membrane. Because the majority of bioavailable iron in mammals exists in the form of heme (iron-protoporphyrin IX), most pathogens also utilize heme-dependent iron-uptake proteins.[4] Heme receptor proteins in the outer membrane accept heme directly or from hemoglobin and transfer it into the cell periplasm.[5,6] From there, periplasmic heme binding proteins carry heme to inner membrane receptors that transfer heme across the inner membrane into the cytoplasm. In the cytoplasm, the porphyrin ring of heme is oxidized and broken to release iron.

Vibrio cholerae, a Gram-negative bacteria, is the causative agent of the diarrheal disease cholera.[7] Based on the genome sequence of *V. cholerae* and bioinformatics-based predictions, putative genes encoding heme-acquisition proteins have been identified and termed Hut (Heme utilization) proteins (Figure 1).[8,9] The outer-membrane heme receptor proteins, HutA, HutR and HasR, transfer heme into the periplasm.[8,10] In the periplasm, the heme-binding protein, HutB, binds to heme, and transfers it to the inner-membrane HutC-HutD protein complex. HutC/HutD in turn transfers heme into the cytoplasm across the inner membrane.[9] In cytoplasm, HutX functions as a heme transport protein to a HutZ,[11] which degrades heme to β- or δ-biliverdin in vitro.[12,13]

A sequence search using BLAST (http://blast.ncbi.nlm.nih.gov/Blast.cgi) revealed several proteins homologous to HutB from *V. cholerae*, namely PhuT from *Pseudomonas aeruginosa*, HmuT from *Yersinia pestis*, and ShuT from *Shigella dysenteriae* (Figure S1). HutB is a putative heme-binding protein in the *V. cholerae* heme-uptake system. In this study, we spectroscopically characterized the heme binding properties and coordination structure of HutB. We found that HutB binds approximately 1 molar equivalent of heme with relatively low affinity, and showed that Tyr65, Tyr198, and His164 are involved in the coordination of heme. HutB possesses the similar coordination structure of heme as that of the cytoplasmic heme-transport protein, HutX, from *V. cholerae* in spite of no sequence and structural homology.[11], indicating that HutB functions as a periplasmic heme-transport protein
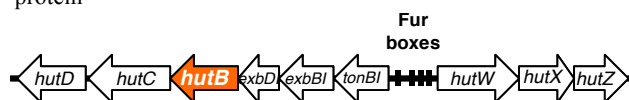

Figure 1. Gene map of the *V. cholerae hut* operon.

2. Experimental

2.1 Materials. The chemicals used in this study were purchased from Wako Pure Chemical Industries (Osaka, Japan), Nacalai Tesque (Kyoto, Japan) or Sigma-Aldrich (St. Louis, MO, USA), and were used without further purification.

2.2 Protein expression and purification. An expression plasmid for the *hutB* gene was purchased from the PlasmID Repository (http://plasmid.med.harvard.edu/PLASMID/Home.xhtml; clone ID VcCD00027319). The *hutB* gene lacking 23 N-terminal residues was amplified by PCR and cloned into a mutated pET-28b vector (Merck Chemicals, Darmstadt, Germany) via *Nde*I and *Eco*RI restriction sites in which the thrombin recognition site (Leu-Val-Pro-Arg-Gly-Ser) was mutated to the HRV 3C protease recognition site (Leu-Glu-Val-Leu-Phe-Gln-Gly-Pro) as described previously.[14] *Escherichia coli* strains carrying expression plasmids for His-tagged HutB protein were grown at 37 °C in LB broth supplemented with 50 μg/ml kanamycin. Expression of the His-HutB fusion protein in *E. coli* BL21(DE3) was induced by

adding isopropyl-β-D-thiogalactopyranoside to a final concentration of 0.4 mM after cultures had reach an optical density at 600 nm (OD_{600}) of 0.6–1.0, and then incubating at 28 °C overnight. Cells were harvested by centrifugation, and the resulting cell pellet was suspended in lysis buffer (50 mM Tris-HCl pH 8.0, 150 mM NaCl, 0.1% Nonidet P-40) and incubated with 1 mg/mL lysozyme and DNase on ice for 60 minutes. The sample was centrifuged at 40,000 × g for 30 minutes, and His$_6$-tagged HutB was purified by affinity chromatography on a HisTrap HP column (GE Healthcare, Uppsala, Sweden). Eluted HutB was incubated with Turbo3C protease (Accelagen, San Diego, CA, USA) for ~16 hours at 4 °C to remove the His$_6$-tag. After cleavage, the reaction mixture was again applied to the HisTrap column. The column flow-through containing untagged HutB was applied to a gel-filtration column (HiLoad 16/60 Superdex 200 pg; GE Healthcare) equilibrated with 50 mM Tris-HCl/150 mM NaCl (pH 8.0). Protein purity was assessed by sodium dodecyl sulfate-polyacrylamide gel electrophoresis (SDS-PAGE) on 12.5% polyacrylamide gels.

Mutagenesis was conducted utilizing a PrimeSTAR mutagenesis basal kit from Takara Bio (Otsu, Japan). DNA oligonucleotides were purchased from Eurofins Genomics (Tokyo, Japan). The mutated genes were sequenced (Eurofins Genomics) to ensure that only the desired mutations were introduced.

2.3 Measurement of heme binding. Heme binding was tracked by difference spectroscopy in the Soret region of the UV-visible spectrum. Aliquots of 0.5 mM hemin in 0.1 M NaOH were added to both the sample cuvette containing 5 μM HutB and reference cuvette containing buffer only. No pH change in the medium was observed after the addition of the hemin solution. Spectra were recorded 3 minutes after addition of each heme aliquot. The absorbance differences at 372 and 407 nm were plotted against the heme concentration.

2.4 Measurement of heme dissociation rate. The heme dissociation rate from HutB was measured in a reaction solution containing 2.0 μM heme-HutB and 20 μM apomyoglobin, prepared by extracting heme using the acid/butanone method,[15] in 50 mM Tris-HCl/150 mM NaCl (pH 8.0) using a stopped-flow apparatus (Unisoku, Osaka, Japan) by following the increase in absorbance at 410 nm. The presence of free hemin was precluded by reconstituting only 0.2 molar equivalents of hemin with 1 molar equivalent of HutB. Further addition of apomyoglobin did not affect the dissociation rate constants. Rate constants were calculated by fitting the data to a single-exponential equation using Igor Pro (WaveMetrics, Portland, OR, USA).

2.5 Spectroscopy. Optical spectra of the purified protein were recorded using a V-660 (Jasco, Tokyo, Japan) UV-visible spectrophotometer at room temperature. Resonance Raman spectra were obtained using a single monochromator (SPEX500M; Jobin Yvon, Edison, NJ, USA) equipped with a liquid nitrogen-cooled CCD detector (Spec-10:400B/LN; Roper Scientific, Princeton, NJ, USA). The excitation wavelengths employed were 413.1 and 441.6 nm, delivered by krypton ion (BeamLok 2060; Spectra Physics, Santa Clara, CA, USA) and helium-cadmium (IK5651R; Kimmon Koha, Tokyo, Japan) lasers, respectively. The laser power at the sample point was adjusted to ~5 mW for the ferric and ferrous forms, and to 0.1 mW for the CO-bound form to prevent photodissociation. Raman shifts were calibrated using indene, CCl_4, acetone, and an aqueous solution of ferrocyanide. The accuracy of the peak positions of well-defined Raman bands was ±1 cm^{-1}. The sample concentration for Raman experiments was about 10 μM in 50 mM Tris-HCl/150 mM NaCl (pH 8.0).

Circular dichroism (CD) spectra in the far-UV region were measured with a J-1500 CD spectrometer (Jasco) over the spectral range of 200 to 250 nm at room temperature. The sample concentration was 5 μM in 50 mM sodium phosphate buffer (pH 8.0) containing 150 mM NaCl. CD spectra were recorded using a quartz cell with a path length of 10 mm. The α-helical content was calculated from the mean residue ellipticity [θ] at 222 nm using the following equation:[16]

$$\alpha\text{-helical (\%)} = (-([\theta]_{222} + 2340)/30300) \times 100 \quad (1)$$

2.6 Size-exclusion chromatography. The oligomerization status of the protein was analyzed using an ENrich SEC 650 gel-filtration column (Bio-Rad, Hercules, CA, USA) equilibrated in 50 mM Tris-HCl/150 mM NaCl (pH 8.0). The elution profile was monitored at 280 and 400 nm. Standards with a known molecular mass (ribonuclease A 13,700 Da; chymotrypsinogen A 25,000 Da; ovalbumin 43,000 Da; bovine serum albumin 66,000 Da; aldolase 158,000 Da; catalase 232,000 Da; ferritin 440,000 Da; thyroglobulin 669,000 Da; and blue dextran 2,000 kDa) (GE Healthcare) were applied to the column.

3. Results and Discussion

3.1 Expression and purification of VcHutB. SOSUI (http://harrier.nagahama-i-bio.ac.jp/sosui/)[17] and SignalP (http://www.cbs.dtu.dk/services/SignalP/)[18] predicated that the N-terminal region of HutB from *V. cholerae* is a periplasmic leader sequence containing a proteolytic cleavage site between amino acid 22 and 23. Accordingly, for this study, we constructed a truncated HutB gene containing residues 23–277, termed VcHutB. The purified protein was verified by SDS-PAGE to be approximately 95% pure, and migrated as a single band with a molecular mass of about 25 kDa (Figure 2A), in good agreement with the calculated molecular mass of VcHutB (27 kDa). An analysis using size-exclusion chromatography indicated that the purified protein was a monomer (~30 kDa) (Figure 2B). This result is in contrast to that obtained for the full-length protein, which eluted in the void volume of the column (Figure 2B).
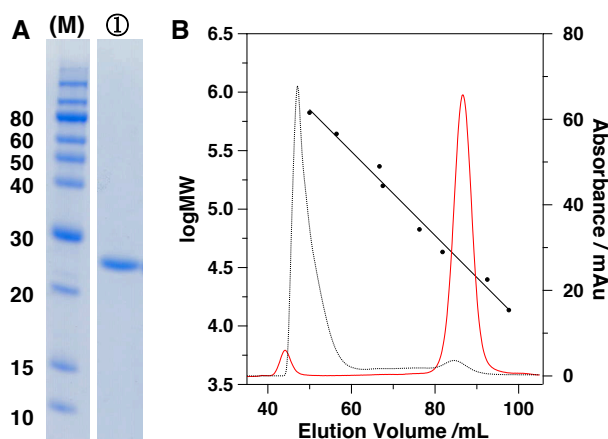

Figure 2. Purification of VcHutB. (A) SDS-PAGE gel of purified VcHutB (lane 1) and molecular mass markers (lane M). (B) Gel-filtration elution profile of VcHutB (red) and full-length HutB (black, dotted) on a Superdex 200 pg column equilibrated with Tris-HCl/150 mM NaCl (pH 8.0). The elution volume for standard proteins was as follows: thyroglobulin, 50.0 mL; ferritin, 56.4 mL; catalase, 66.7 mL; aldose, 67.5 mL; albumin, 76.3 mL; ovalbumin, 81.8 mL; chymotrypsinogen A, 92.5 mL; and RNase A, 97.6 mL.

Although the pellet of VcHutB-expressing cells was brownish-red, the purified protein was colorless, suggesting

that *Vc*HutB was present as an apoprotein with no endogenous heme content after purification. Addition of an aliquot of hemin to the apoprotein yielded a solution with a broad Soret band at approximately 380 nm, which is different from that of free hemin (λ_{max} ~386 nm). To confirm the heme-binding ability of *Vc*HutB, we determined the stoichiometry of heme binding to *Vc*HutB. *Vc*HutB at a fixed concentration was titrated with increasing amounts of heme. The absorption spectra at different concentrations of heme are shown in Figure 3A. The absorbance difference between the solution containing the apoprotein and buffer alone titrated with heme was plotted against the heme concentration (Figure 3B). The absorbance at 404 nm increased with an increase in the heme concentration to 0.5 equivalents, and then decreased up to 1.0 equivalent; no further change was observed beyond 1.0 equivalent of added heme. In contrast, absorbance at 373 nm did not change until reaching 0.5 heme equivalents, and then increased, plateauing at 1.0 equivalent as observed for the absorbance change at 407 nm. These spectral changes are quite unusual for a heme titration plot and could not readily be fit to a sigmoidal curve. Therefore, the binding stoichiometry was not determined. However, we concluded that at least 0.5 equivalents of heme bind to *Vc*HutB, and the coordination structure undergoes a change at more than 0.5 equivalents.
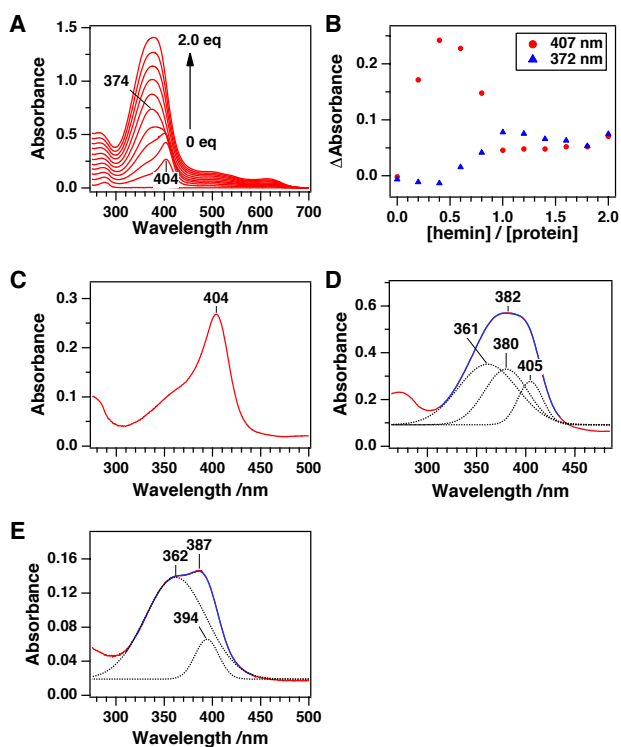

Figure 3. Optical absorbance spectrum of heme complexes of *Vc*HutB. (A) Absorption spectra of *Vc*HutB (10 μM) titrated with heme from 0 to 2.0 equivalents at 0.2-equivalent intervals. (B) The absorbance difference at 372 nm (blue triangle) and 407 nm (red circle) following stepwise addition of heme (1–20 μM) to *Vc*HutB (10 μM). Deconvolution of absorption spectra of (C) 0.2eq-heme-*Vc*HutB, (D) 0.8eq-heme-*Vc*HutB, and (E) hemin. All samples were in 50 mM Tris-HCl/150 mM NaCl (pH 8.0).

3.2 UV-visible absorption spectra of heme-reconstituted *Vc*HutB. To determine the coordination structure of the heme complex of *Vc*HutB, we measured the UV-visible absorption spectra. The absorption spectrum of

*Vc*HutB reconstituted with 0.2 equivalents of heme (hereafter termed 0.2eq-heme-*Vc*HutB) is shown in Figure 2C. A sharp Soret band appeared at 404 nm, which is similar to that observed for catalase[19] and peroxidases,[20] indicating that tyrosine or histidine is a heme ligand of 0.2eq-heme-*Vc*HutB.

Addition of 0.8 equivalents of heme to *Vc*HutB (0.8eq-heme-*Vc*HutB) produced a Soret band that was broader and blue-shifted (382 nm) compared with that of 0.2eq-heme-*Vc*HutB (Figure 3D). The spectrum in the Soret region was fitted with Gaussian functions. A good fit was achieved by three components with maxima at 361, 380, and 405 nm (Figure 3D). The 361- and 380-nm species were not observed in 0.2eq-heme-*Vc*HutB (Figure 3C). To assign these two bands, we analyzed the absorption spectrum of free hemin. The broad Soret band was deconvoluted into two distinct bands at 362 and 394 nm (Figure 3E). This spectrum suggests that the 361-nm species of the 0.8eq-heme-*Vc*HutB is derived from free heme, or heme that was loosely associated with the protein.

3.3 Resonance Raman spectra of heme-reconstituted *Vc*HutB. To further confirm the coordination structure of heme-*Vc*HutB, we measured resonance Raman spectra. Resonance Raman spectra of 0.2eq-heme-*Vc*HutB are shown in Figure 4A. The spin-state marker band, ν_3, which is observed at
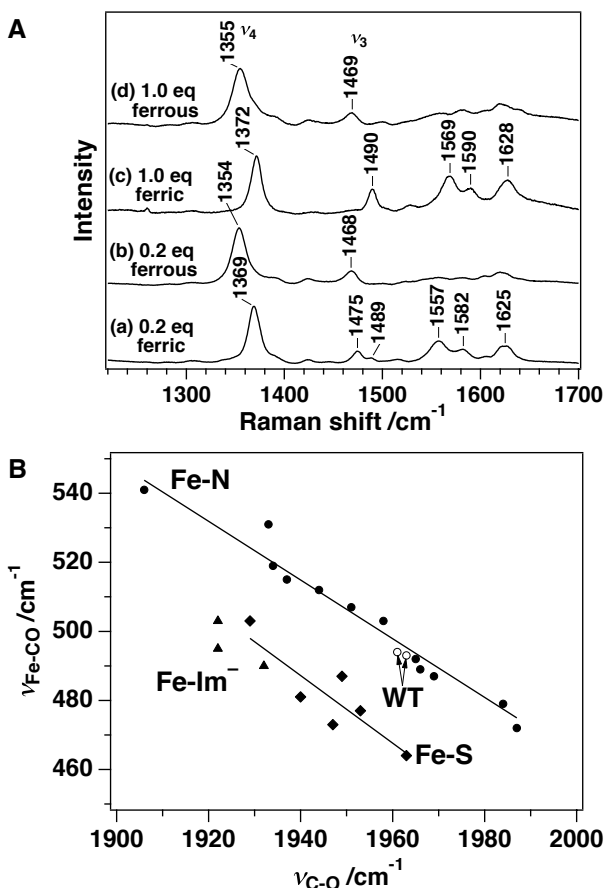

Figure 4. (A) Resonance Raman spectra of heme-*Vc*HutB in Tris-HCl/150 mM NaCl (pH 8.0) excited at 413.1 nm; (a) ferric 0.2eq-heme-*Vc*HutB, (a) ferrous 0.2eq-heme-*Vc*HutB, (b) ferric 1.0eq-heme-*Vc*HutB, and (d) ferrous 1.0eq-heme-*Vc*HutB. (B) Correlation plot between frequencies of ν_{Fe-CO} and ν_{C-O} stretching modes. The two solid lines correspond to correlations for proteins with proximal imidazoles (solid circles), proximal imidazolates (solid triangles), and thiolate-ligated hemoproteins (solid diamonds). The data points for heme-*Vc*HutB are presented as open circles.

1480–1510 cm⁻¹ for most heme proteins,[21] appeared at 1475 cm⁻¹, characteristic of a 6-coordinate high-spin heme (spectrum a). The small peak at 1489 cm⁻¹ corresponds to a 5-coordinate high-spin heme. Upon reduction, the ν_3 band shifted to 1468 cm⁻¹, which is characteristic of a 5-coordinate high-spin heme (Figure 4A, spectrum b).

Reconstitution of VcHutB with 1.0 equivalent of heme yielded a resonance Raman spectrum for the ferric form that was quite different from that of 0.2eq-heme-VcHutB. The ν_3 band appeared at 1490 cm⁻¹ (Figure 4A, spectrum c), a frequency that suggests that the ferric heme is in a 5-coordinate high-spin state. Furthermore, the relatively larger ratio of the intensity of the ν_4 band (1372 cm⁻¹) to that of the ν_3 band indicates coordination of an anionic ligand such as tyrosine, cysteine or OH⁻, but not histidine, to the heme iron.[22,23] For ferrous 1.0eq-heme-VcHutB, the ν_3 band at 1469 cm⁻¹ band is derived from the 5-coordinate high-spin heme (Figure 4A, spectrum d).

Two isotope-sensitive bands appeared at 493–494 and 1961–1963 cm⁻¹ in the CO-bound form of VcHutB reconstituted with either 0.2 or 1.0 equivalents of heme (Figure S2). The 493–494 and 1961–1963 cm⁻¹ bands were assigned to Fe-CO (ν_{Fe-CO}) and C-O (ν_{C-O}) stretching modes, respectively, on the basis of substitutions with ¹³C¹⁸O. The position of the frequencies of ν_{Fe-CO} and ν_{C-O} on the correlation plot of ν_{Fe-CO} versus ν_{C-O} provides useful insight into the donor strength of the trans ligand of iron-bound CO.[24,25] The plot for heme-VcHutB fell on the line with proteins that possess neutral histidine as a heme ligand (Figure 4B).

3.4 Heme binding site of VcHutB. A comparison of the amino acid sequence of VcHutB to that of HmuT from *Yersinia pestis*, whose crystal structure has been reported,[26] suggests that Tyr65, Tyr198, and His164 are possible heme ligands (Figure S1). Therefore, we individually mutated each of the tyrosines to phenylalanine, and the histidine to alanine. The absorption spectrum of the H164A mutant in the presence of 0.2 equivalents of heme (Figure 5A) was substantially different from that of 0.2eq-heme-VcHutB (Figure 3C). The broad Soret band at 389 nm in this spectrum is somewhat similar to that of 0.8eq-heme-VcHutB (Figure 3D). A deconvolution analysis of the heme-H164A mutant spectrum revealed that the Soret band consists of three bands with maxima at 364, 387, and 404 nm.

The presence of the 404-nm species in the H164A mutant indicates that coordination of heme for the 404-nm species does not involve His164. The 364-nm species for the heme-H164A mutant corresponded to that of the dominant free hemi component (Figure 3E), even though only 0.2 equivalents of hemin was added. The presence of a free hemin component indicates that mutation of His164 led to a significant decrease in the affinity for heme.

Replacement of Tyr65 with phenylalanine resulted in a blue shift of the Soret band to 390 nm, with a shoulder at around 365 nm (Figure 5B). Although this spectrum is similar to that of free hemin (Figure 3E), it closer to that of the heme complex of HutX from *V. cholerae*, whose heme ligand is Tyr90.[11] This implies that tyrosine coordinates with heme in the Y65F mutant. The Soret band of the 0.2eq-heme-Y198F mutant was also blue-shifted to 381 nm compared with that of 0.2eq-heme-VcHutB (Figure 5C). The shape of the Soret band was slightly different from that of the heme-Y65F mutant. Deconvolution of the broad Soret band of the 0.2eq-heme-Y198F mutant into two Gaussian components yielded two peaks at 366 and 396 nm, which are the same as those observed in the 0.2eq-heme-Y65F mutant (Figure 5B). This analysis suggests that the different shape of the Soret band of the 0.2eq-heme-Y198F mutant is attributable to the difference in the ratio between the 365-nm species and the 396-nm species. The smaller ratio of the 396-nm species to the 365-nm species in the Y198F mutant indicates that the affinity of heme for the Y198F mutant is slightly lower than that for the Y65F mutant, because the 365-nm species corresponds to the 361-nm species of the 0.8eq-heme-VcHutB Wild Type (WT).

3.5 Heme dissociation rate of VcHutB. To further confirm the heme ligand of VcHutB, we measured the heme-dissociation rate constant, $k_{off,heme}$, which provides information about the heme axial ligand: the $k_{off,heme}$ for myoglobin, which possesses histidine as a heme ligand, is on the order of 10^{-7} s⁻¹,[27] whereas that for HutX, which possesses tyrosine as a heme ligand, is on the order of 10^{-3} s⁻¹.[11] The $k_{off,heme}$ for 0.2eq-heme-VcHutB was obtained by adding a 10-fold molar excess of apomyoglobin to a solution containing heme-VcHutB and monitoring the time course of heme transfer from VcHutB to apomyoglobin at 410 nm (Figure 6). The data were well fit to a single-exponential function, which yielded a $k_{off,heme}$ of $(4.8 \pm 0.3) \times 10^{-2}$ s⁻¹. This value is close to that for HutX rather than that for myoglobin, supporting the conclusion that the heme ligand of VcHutB is tyrosine, and not histidine.
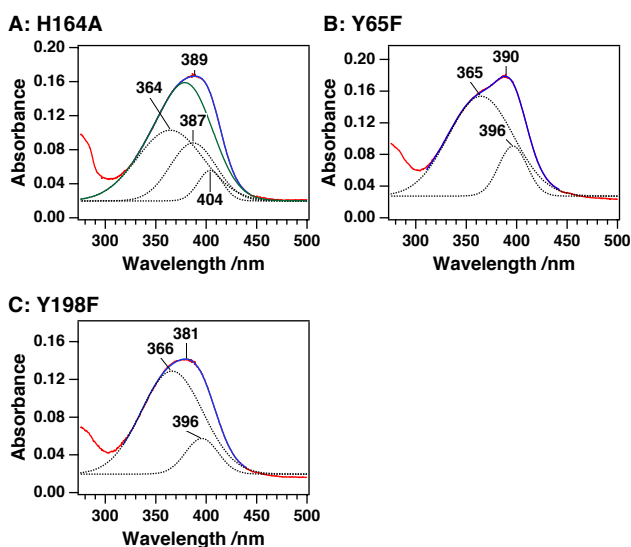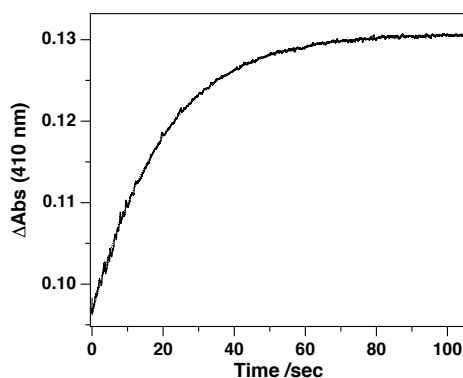

Figure 5. Optical absorption spectra of (A) 0.2eq-heme-H164A, (B) 0.2eq-heme-Y65F, and (C) 0.2eq-heme-Y198F. All samples were in 50 mM Tris-HCl/150 mM NaCl (pH 8.0).

Figure 6. Dissociation of heme from the heme-VcHutB complex. Time course of the displacement of hemin from heme-VcHutB to apomyoglobin. The reaction was monitored after initiation of the reaction by manually mixing heme-VcHutB (2.0 μM) with apomyoglobin (20 μM) in 50 mM Tris-HCl/150 mM NaCl (pH 8.0).

3.6 Secondary structure of *Vc*HutB. To estimate the secondary structure change induced by heme binding to *Vc*HutB, we measured far-UV CD spectra (Figure 7). The CD spectrum of *Vc*HutB has a characteristic feature with a minimum at 222 nm, a negative shoulder at 209 nm and a maximum at 193 nm, indicating that the protein is rich in α-helical structure.[16] Addition of up to 2 equivalents of heme to *Vc*HutB did not affect the far-UV CD spectrum, indicating that binding of heme to *Vc*HutB induced no appreciable rearrangement of the secondary structure.

Figure 7B shows CD spectra of the *Vc*HutB mutants. Mutation of Tyr65 to phenylalanine caused no spectral change, except a slight decrease in intensity. In contrast, mutation of His164 or Tyr198 altered CD spectra, causing merging of the negative peak at 209 and 222 nm into a broad peak at 220 nm. This change suggests that His164 and Tyr198 mutations cause a slight perturbation in the secondary structure, indicating that these residues are important for maintaining the secondary structure of *Vc*HutB.
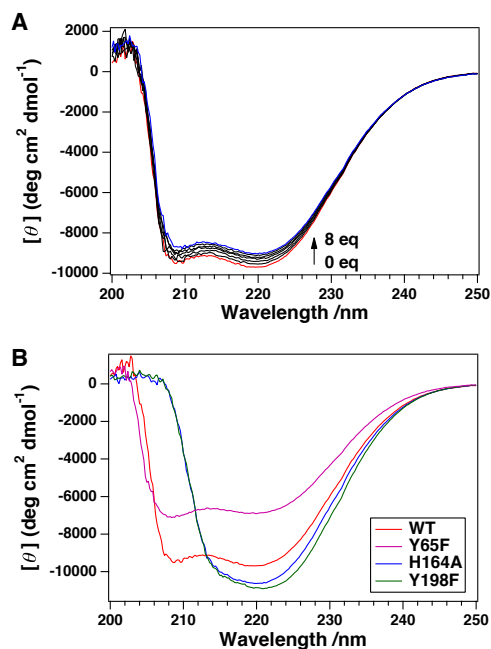

Figure 7. Effects on CD spectra of heme binding to *Vc*HutB. (A) CD spectra in the far-UV region of 3 μM *Vc*HutB containing no heme, and 1, 2, 4, or 8 equivalents of heme in 50 mM sodium phosphate (pH 8.0). (B) CD spectra of WT *Vc*HutB and H164A, Y65F, and Y198F mutant *Vc*HutB.

3.7 Coordination structure of heme bound to *Vc*HutB. *Vc*HutB was a suspected heme transport protein based on its sequence homology to HmuT from *Y. pestis* (Figure S1).[26] Indeed, *Vc*HutB-expressing cell pellets were reddish-brown, suggesting that *Vc*HutB expressed in *E. coli* contains heme. However, the purified protein was colorless, and thus devoid of heme. Titration of *Vc*HutB with heme showed that at least 0.5 equivalents of heme bind to *Vc*HutB. The absorption spectra suggest that the dominant component at lower heme concentrations (<0.5 equivalents) is the 404-nm species (Figure 3C), but it is converted to a different species with a Soret maximum at 382 nm at higher heme concentrations (>0.5 equivalents) (Figure 3D). One possible explanation for this conversion is that heme binds to the dimer interface, as observed for ChaN from *Campylobacter jejuni*.[28] However, this

could not be the case, because *Vc*HutB is a monomer even after reconstitution with heme (Figure S3). The Soret maximum at 404 nm of 0.2eq-heme-*Vc*HutB implies an H_2O-bound 6-coordinate heme with tyrosine as a heme ligand (Figure 3C), as observed in catalase[19] and CcmE,[22] or with histidine, as observed in heme peroxidase.[20] The mutational study suggests that His164 is not necessary for formation of the 404-nm species (Figure 5A), a conclusion supported by the observation that this residue is not conserved (Figure S1). Thus, tyrosine, but not histidine, is likely a heme ligand of *Vc*HutB. For 0.8eq-heme-*Vc*HutB, 5-coordinate heme was dominant (Figures 3D and 4A). Therefore, at higher concentrations of heme, the sixth ligand might be released from the heme to form a 5-coordinate heme for reasons that are currently unknown.

Another possibility is ligand dissociation/association, depending on the heme concentration. At lower concentrations of heme, both Tyr65 and Tyr198 would coordinate to heme, whereas one of Tyr would dissociate from heme to be 5-coordinate at higher concentrations of heme. In the heme titration experiment of HmuT from *Y. pestis*, absorbance at 404 nm increased up to 1 equivalent of heme, and then absorbance at 373 nm increased, indicating that the heme is 6-coordinate at lower concentrations of heme, whereas it is 5-coordinate at higher concentrations of heme.[26] Crystal structure of 2 equivalents of heme-bound HmuT showed that two stacked hemes were 5-coordinated by tyrosine or histidine in the heme binding site.[26] Because the same trend was observed, the geometry change depending on the heme concentration seems to be common in some kinds of periplasmic heme binding proteins.

Unfortunately, we could not obtain heme affinity of each coordination structure (Figure 3B). Thus, it is difficult to determine the biological significance of the geometry change of heme. This geometry change observed in *Vc*HutB might be correlated with heme transport efficiency, because heme affinity would be related with the coordination number of heme. Thus, we predicted that *Vc*HutB transfers heme more or less efficiently under the lower heme concentration, and vice versa.

Mutation of His164 to alanine significantly increased the 364-nm species component, which corresponds to free hemin, even at a heme-to-protein ratio of 0.2 (Figure 5A). This result also indicates that His164 is not a heme ligand, but helps tyrosine to bind heme. The role of histidine in assisting Tyr-coordination is also seen in hemophore proteins such as HasA.[29] Structural characterizations of HasA from *S. marcescens* have revealed that Tyr75 and His32 are bound to heme. His83 forms a hydrogen bond with Tyr75,[30] and mutation of His83 with alanine causes a drastic decrease in the affinity for heme.[29] Therefore, His83 is essential for heme binding to HasA, but not to the heme ligand. Collectively, the observations suggest that His164 in *Vc*HutB plays a key role in heme ligation comparable to that of His83 in HasA.

Heme-bound forms of the Y65F and Y198F mutants exhibited different absorption spectra from that of WT *Vc*HutB (Figure 5B, 5C). The Soret band of both mutants contained two components with maxima at 366 and 396 nm. The latter peak is close to that observed for proteins possessing tyrosine as an axial ligand, such as RV0203 (392 nm),[31] HutX (390 nm),[11] and PGRMC1 (400 nm).[32] Because Tyr65 and Tyr198 are predicted to be located close to each other based on crystal structures of homologous proteins,[28] heme can still bind to a protein in which one of the tyrosine residues is replaced. Therefore, we could not determine the heme ligand of WT *Vc*HutB based on the mutational study. However, it is certain that both Tyr65 and Tyr198 are involved in heme binding to *Vc*HutB.

3.8 Functional aspects of *Vc*HutB. The first 22 amino acid residues of *Vc*HutB were predicted to comprise a leader sequence that directs the protein to the periplasmic space. The full-length protein with the leader sequence was eluted in the void volume of the Superdex 200 column (Figure 2B), indicating the formation of soluble aggregates. In contrast, the protein without the leader sequence exists in a monomeric form (Figure 2B). Therefore, the leader sequence would be cleaved when it translocates into the outer-membrane, consistent with the function of *Vc*HutB as a soluble periplasmic protein. Although the exact heme affinity for *Vc*HutB could not be calculated from the heme-titration plot owing to its strange behavior (Figure 3B), the affinity was not particularly strong, considering that the protein was purified as an apoprotein and a free heme component was detected for 0.8eq-heme-HutB (Figure 3D). This moderate heme-affinity is attributable to the coordination structure of *Vc*HutB. As described above, either Tyr65 or Tyr198 is a heme ligand. The heme dissociation rate, $k_{off,heme}$, for proteins with Tyr-coordination tends to be larger than that for proteins with His coordination. Indeed, the $k_{off,heme}$ for 0.2eq-heme-*Vc*HutB was much larger than that for myoglobin, but comparable to that for HutX (Figure 6).[11] Tyrosine is a weaker heme ligand than histidine, as observed in other heme transport proteins such as HasA and Isd.[33] However, it is suitable for heme transport proteins because it allows rapid heme dissociation. Hut proteins from *V. cholerae* contain two heme-transport proteins: HutB and HutX (Figures 1, 8). Although there is no sequence homology between HutB and HutX, the heme ligand of both proteins is tyrosine, and a nearby histidine is involved in heme binding. This geometry is suitable for efficient heme transfer.
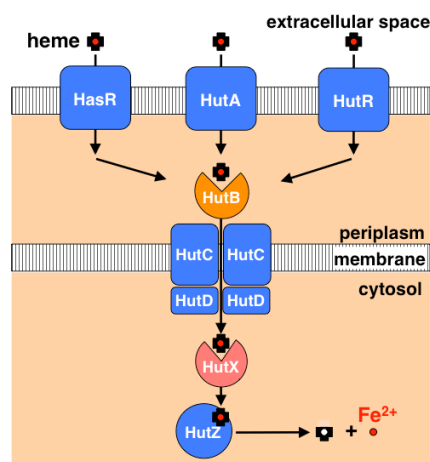

Figure 8. Schematic representation of heme uptake system of *V. cholerae*.

4. Conclusion

HutB from *V. cholerae* specifically binds to heme through Tyr65 or Tyr198, and His164 is involved in heme binding. *Vc*HutB utilizes the same heme coordination structure as HutX, the cytosolic heme-transport protein in *V. cholerae*.

References

1   S. C. Andrews, A. K. Robinson, F. Rodríguez-Quiñones, *FEMS Microbiol. Rev.* **2003**, *27*, 215.

2   H. Contreras, N. Chim, A. Credali, C. W. Goulding, *Curr. Opin. Chem. Biol.* **2014**, *19*, 34.

3   V. Braun, H. Killmann, *Trends Biochem. Sci.* **1999**, *24*, 104.

4   C. Wandersman, I. Stojiljkovic, *Curr. Opin. Microbiol.* **2000**, *3*, 215.

5   V. Braun, K. Hantke, *Curr. Opin. Chem. Biol.* **2011**, *15*, 328.

6   Y. Tong, M. Guo, *Arch. Biochem. Biophys.* **2009**, *481*, 1.

7   J. B. Kaper, J. G. Morris, M. M. Levine, *Clin. Microbiol. Rev.* **1995**, *8*, 48.

8   E. E. Wyckoff, A. R. Mey, S. M. Payne, *Biometals* **2007**, *20*, 405.

9   E. E. Wyckoff, M. Schmitt, A. Wilks, S. M. Payne, *J. Bacteriol.* **2004**, *186*, 4142.

10   A. R. Mey, S. M. Payne, *Mol. Microbiol.* **2001**, *42*, 835.

11   Y. Sekine, T. Tanzawa, Y. Tanaka, K. Ishimori, T. Uchida, *Biochemistry* **2016**, *55*, 884.

12   T. Uchida, Y. Sekine, T. Matsui, M. Ikeda-Saito, K. Ishimori, *Chem. Commun.* **2012**, *48*, 6741.

13   N. Dojun, Y. Sekine, K. Ishimori, T. Uchida, *Dalt. Trans.* **2017**, *46*, 5147.

14   T. Uchida, M. Sasaki, Y. Tanaka, K. Ishimori, *Biochemistry* **2015**, *54*, 6610.

15   F. W. Teale, *Biochim. Biophys. Acta* **1959**, *35*, 543.

16   Y.-H. H. Chen, J. T. Yang, H. M. Martinez, *Biochemistry* **1972**, *22*, 4120.

17   T. Hirokawa, S. Boon-Chieng, S. Mitaku, *Bioinformatics* **1998**, *14*, 378.

18   T. N. Petersen, S. Brunak, G. von Heijne, H. Nielsen, *Nat. Methods* **2011**, *8*, 785.

19   A. S. Brill, R. J. Williams, *Biochem. J.* **1961**, *78*, 253.

20   H. B. Dunford, J. S. Stillman, *Coord. Chem. Rev.* **1976**, *19*, 187.

21   T. G. Spiro, X. Y. Li, in *Biological Applications of Raman Spectroscopy*, III ed., ed. by T. G. Spiro, John Wiley and Sons, New York, **1988**, pp. 1–37.

22   T. Uchida, J. M. Stevens, O. Daltrop, E. M. Harvat, L. Hong, S. J. Ferguson, T. Kitagawa, *J. Biol. Chem.* **2004**, *279*, 51981.

23   S. Eakanunkul, G. S. Lukat-Rodgers, S. Sumithran, A. Ghosh, K. R. Rodgers, J. H. Dawson, A. Wilks, *Biochemistry* **2005**, *44*, 13179.

24   G. B. Ray, X. Y. Li, J. A. Ibers, J. L. Sessler, T. G. Spiro, *J. Am. Chem. Soc.* **1994**, *116*, 162.

25   T. G. Spiro, I. H. Wasbotten, *J. Inorg. Biochem.* **2005**, *99*, 34.

26   D. Mattle, A. Zeltina, J. S. Woo, B. A. Goetz, K. P. Locher, *J. Mol. Biol.* **2010**, *404*, 220.

27   M. S. Hargrove, D. Barrick, J. S. Olson, *Biochemistry* **1996**, *35*, 11293.

28   A. C. K. Chan, B. Lelj-Garolla, F. I. Rosell, K. A. Pedersen, A. G. Mauk, M. E. P. Murphy, *J. Mol. Biol.* **2006**, *362*, 1108.

29   C. Deniau, R. Gilli, N. Izadi-Pruneyre, S. Létoffé, M. Delepierre, C. Wandersman, C. Briand, A. Lecroisey,

Biochemistry **2003**, *42*, 10627.

30   P. Arnoux, R. Haser, N. Izadi, A. Lecroisey, M. Delepierre, C. Wandersman, M. Czjzek, *Nat. Struct. Biol.* **1999**, *6*, 516.

31   C. P. Owens, J. Du, J. H. Dawson, C. W. Goulding, *Biochemistry* **2012**, *51*, 1518.

32   Y. Kabe, T. Nakane, I. Koike, T. Yamamoto, Y. Sugiura, E. Harada, K. Sugase, T. Shimamura, M. Ohmura, K. Muraoka, A. Yamamoto, T. Uchida, S. Iwata, Y. Yamaguchi, E. Krayukhina, M. Noda, H. Handa, K. Ishimori, S. Uchiyama, T. Kobayashi, M. Suematsu, *Nat. Commun.* **2016**, *7*, 11030.

33   J. C. Grigg, G. Ukpabi, C. F. M. Gaudin, M. E. P. Murphy, *J. Inorg. Biochem.* **2010**, *104*, 341.